

THE VERY FAINT *K*-BAND AFTERGLOW OF GRB 020819 AND THE DUST EXTINCTION HYPOTHESIS OF THE DARK BURSTS

S. KLOSE,¹ A. A. HENDEN,² J. GREINER,³ D. H. HARTMANN,⁴ N. CARDIEL,⁵ A. J. CASTRO-TIRADO,⁶ J. M. CASTRO CERÓN,⁷
J. GALLEGO,⁵ J. GOROSABEL,^{8,9} B. STECKLUM,¹ N. TANVIR,¹⁰ U. THIELE,¹¹ F. J. VRBA,² AND A. ZEH¹

Received 2003 February 8; accepted 2003 April 15

ABSTRACT

We report rapid follow-up *K'*-band observations of the error box of the bright *High Energy Transient Explorer* burst GRB 020819. We find that any afterglow was fainter than $K' = 19$ only 9 hr after the burst. Because no optical afterglow was found, GRB 020819 represents a typical “dark burst.” At first, we discuss if extinction by cosmic dust in the GRB host galaxy could explain the faintness of the afterglow of GRB 020819. We then turn to the entire ensemble of *K*-band dark afterglows. We find that extinction by cosmic dust in the GRB host galaxies is still a possible explanation for the faintness of many afterglows. In all investigated cases a combination of only a modest extinction with a modest redshift can explain the observations. However, the required extinction is very high if these bursts occurred at redshifts smaller than unity, perhaps arguing for alternative models to explain the nature of the dark bursts.

Subject headings: gamma rays: bursts — infrared: general

1. INTRODUCTION

The discovery of optical afterglows of gamma-ray bursts (GRBs) led to a major breakthrough in our understanding of this phenomenon and established a worldwide effort to detect and follow afterglows in many wavebands and over periods as long as a year. By the end of 2002 about 40 GRB afterglows have been discovered in the optical and partly also in the near-infrared bands (van Paradijs, Kouveliotou, & Wijers 2000).¹² Most of them reached *R*-band magnitudes of about 21 ± 1 one day after the burst and were fading with a typical rate of about 3 mag dex^{-1} in time, roughly corresponding to a t^{-1} decay law for the flux. On the other hand, after the discovery of the first two optical GRB afterglows and the follow-up observations of their light curves (GRBs 970228 and 970508; e.g., van Paradijs et al. 1997; Pedersen et al. 1998), there was some hope that all GRB afterglows would be detectable within the aforementioned magnitude range within 1 day after the burst without being in conflict with unsuccessful searches for GRB afterglows in the 1990th (e.g., Vrba, Hartmann, & Jennings 1995). It turned out, however, that the first two optically identified GRB

afterglows are at the bright end of the afterglow brightness distribution. Since 1997 in several cases response times, Δt , were as short as $\lesssim 0.5$ days, GRB error boxes small (arcminute-sized), and the observations deep ($R > 23$), but still no optical afterglow was found even when sometimes a bright and fading X-ray and/or radio afterglow was detected. The term *dark burst* was created in the literature to describe these optically dim afterglows. GRB 020819 is another member of this phenomenological class.

So far, there is no general consensus on the reason for the nondetections of a large fraction of GRB afterglows in the optical bands (for a discussion see, e.g., Fynbo et al. 2001; Lazzati, Covino, & Ghisellini 2002). The problem is complex, since various factors can come into play. The existence of dark bursts could reflect the spread in the physical parameters that determine the radiation properties of the GRB fireball (e.g., Taylor et al. 2000; Berger et al. 2002a). Moreover, if bursters are associated with massive stars still embedded in star-forming regions, then a large amount of interstellar dust could block the optical flux from the afterglow (Paczynski 1998). Last but not least, the mixing of afterglow properties and observational limits cannot be easily resolved. Finally, various independent studies indicate that the redshift distribution of the burster is very broad, presumably with a large fraction of the burster population located at high redshifts (e.g., Mészáros & Mészáros 1996; Horvath, Mészáros, & Mészáros 1996; Schmidt 2001; Schaefer, Deng, & Band 2001; Bagoly et al. 2002). This suggests that a certain fraction of the dark bursts could be dark because of Lyman absorption in the optical bands by intervening intergalactic Lyman limit systems.

Near-infrared (NIR) observations are particularly suited to test the nature of dark bursts. Since the bulk of the optically detected burster population is at redshifts around 1, with a tail toward higher redshifts, optical observations basically trace the UV properties of the interstellar medium in the GRB host galaxies where the opacity of the cosmic dust is high. Furthermore, if optically dark bursts are actually dark because of intergalactic Lyman absorption, NIR observations could reveal the predicted population of high-redshift afterglows (Lamb & Reichart 2000).

¹ Thüringer Landessternwarte Tautenburg, 07778 Tautenburg, Germany.

² USNO/USRA, US Naval Observatory, Flagstaff Station, Flagstaff, AZ 86002.

³ Max-Planck-Institut für Extraterrestrische Physik, 85741 Garching, Germany.

⁴ Department of Physics and Astronomy, Clemson University, Clemson, SC 29634.

⁵ Universidad de Complutense de Madrid, Spain.

⁶ Instituto de Astrofísica de Andalucía (IAA-CSIC), 18080 Granada, Spain.

⁷ Real Instituto y Observatorio de la Armada, Sección de Astronomía, 11.110 San Fernando-Naval (Cádiz), Spain.

⁸ Laboratorio de Astrofísica Espacial y Física Fundamental, 28080 Madrid, Spain.

⁹ Space Telescope Science Institute, Baltimore, MD 21218.

¹⁰ Department of Physical Sciences, University of Hertfordshire, Hatfield, Herts AL10 9AB, UK.

¹¹ Calar Alto Observatory, E-04004 Almeria, Spain.

¹² See the Web site maintained by J. Greiner, <http://www.mpe.mpg.de/~jcg/grbgen.html>.

In the present paper, we concentrate on those optically dark GRB afterglows that have not been detected in the K band either. Our goal is to explore the consequences of the dust extinction hypothesis of the dark bursts. We assume that these afterglows were predominantly dark because of dust extinction in their host galaxies. We ask what the required extinction would have been in these hosts in order to obscure these afterglows for the observer, not only in the optical bands but even in the K band, where the (redshift-corrected) opacity of this dust should have been substantially reduced. Our starting point is GRB 020819, which was well localized on the sky during its burst phase in the X-ray band but whose afterglow remained undetected in the optical/NIR bands down to deep flux limits.

2. OBSERVATIONS AND DATA REDUCTION

The bright burst 020819 triggered the *High Energy Transient Explorer (HETE)* Freigate instrument in the 30–400 keV band on 2002 August 19 at 14:57:35.28 UT (19.623325 UT; trigger 2275). In the 8–40 keV band, it had a duration of ≈ 20 s and a peak brightness of about 5 crab (Vanderspek et al. 2002). The original error box had a radius of only $7'$. Within the following 3 hr the GRB error box was refined, based on *HETE*'s soft X-ray camera (SXC) data, to a radius of only $r = 130''$, centered at R.A., decl. (J2000) = $23^{\text{h}}27^{\text{m}}24^{\text{s}}$, $6^{\circ}16'08''$ (Vanderspek et al. 2002). Some days later, this box was further reduced by the *HETE* team to an error circle of $64''$ in radius, centered at R.A., decl. (J2000) = $23^{\text{h}}27^{\text{m}}25^{\text{s}}.1$, $6^{\circ}16'46''$ (Crew et al. 2002). The burst was also observed by *Ulysses* and triangulated by the Interplanetary Network (IPN) with the error annulus nearly completely covering the revised *HETE*/SXC error circle (Hurley et al. 2002; Crew et al. 2002; all reported error boxes refer to a 90% confidence circle; Fig. 1¹³). Unfortunately, neither X-ray nor radio follow-up observations have been reported for this burst. We adopt the hypothesis that this was an otherwise bona fide long-duration GRB. This is justified by (1) the spectral properties of the burst, which indicate that the burst was not unusual in any respect compared to other long-duration bursts detected by the *HETE*/Fregate instrument by the end of 2002 (Barraud et al. 2003); (2) the duration of the burst, which clearly indicates that this is a member of the population of the long bursts; and (3) the Galactic coordinates of the burst, which make a Galactic origin less likely.

We started near-infrared imaging of the $r = 130''$ SXC error circle about 8.3 hr after the burst, using the Calar Alto

3.5 m telescope equipped with the Omega Prime near-infrared camera (Henden et al. 2002; Fig. 2). The time delay of 8.3 hr was mainly caused by the visibility of the field on the sky over Calar Alto, Spain. Omega Prime uses a 1024×1024 Hg:Cd:Te array made by Rockwell with a plate scale of $0''.4$ pixel⁻¹. The field of view is $6'.8 \times 6'.8$. For our 1 hr integration time the limiting magnitude of the combined image is about $K' = 19.5$.

The GRB field was observed again at Calar Alto with the same instrumentation 1 day after the first observing run. Finally, third epoch K' -band observations were executed with Omega Prime one week after the burst. Also, the UK Infrared Telescope (UKIRT) equipped with the UKIRT fast-track imager was used to perform follow-up J - and K -band observations 1 day after the burst of a potential afterglow candidate reported by Henden et al. (2002). At a pixel scale of $0''.091$ pixel⁻¹ and a field of view of $92'' \times 92''$, the UKIRT image is about 1 mag deeper than the Calar Alto image and shows the potential afterglow candidate as stellar-like. However, it later turned out that this source lies outside the $64''$ SXC error circle and, furthermore, did not show evidence for variability on deep optical images (Price et al. 2002; Rol et al. 2002). Similarly, we do not detect a K -band counterpart to the potential radio transient reported by Frail & Berger (2003). Additional K -band data were obtained for the revised SXC error circle with the NIR imager SOFI at the ESO NTT 3.5 m telescope at La Silla, Chile, and with ISAAC at the ESO-VLT on Paranal, Chile (Table 1). SOFI is equipped with a 1024×1024 Rockwell Hg:Cd:Te Hawaii array with $18.5 \mu\text{m}$ pixels and a plate scale of $0''.29$ pixel⁻¹, whereas ISAAC makes use of a 1024×1024 pixel Rockwell Hg:Cd:Te array and offers a plate scale of $0''.147$ pixel⁻¹.

In all but one case, standard stars from the list of Persson et al. (1998) were observed. During the first and the second Calar Alto observing run we included Persson's stars 9162 and 9188, respectively. For the NTT/SOFI run the observed stars were 9104 and 9108 and for the VLT/ISAAC run star 9181. No standard star was observed during the third Calar Alto run.

The NIR frames were reduced in standard fashion using three independent procedures based on IRAF (Image Reduction and Analysis Facility distributed by the U.S. National Optical Astronomy Observatory), image reduction routines based on the commercial software IDL, as well as ESO's *eclipse* software collection (Devillard 1997). Since the number of individual frames per observing run was high and a mosaic was taken, in all cases the sky subtraction encountered no problems. For the calibration of the ISAAC image, air-mass correction in the K band was performed

¹³ See the *HETE* Web site at <http://space.mit.edu/HETE/>.

TABLE 1
OBSERVATION LOG OF THE *HETE*/SXC ERROR CIRCLE OF GRB 020819

Epoch (UT)	$\langle \Delta t \rangle^a$	Telescope/Instrument	Filter	Exposure (s)	Air Mass	K Limiting Magnitude
2002 Aug 19.9660–20.0236.....	8.9 hr	CA 3.5 m, Omega Prime	K'	63×60	1.45–1.22	19.5
2002 Aug 20.9660–21.0354.....	1.4 days	CA 3.5 m, Omega Prime	K'	75×60	1.44–1.18	19.5
2002 Aug 25.2771–25.3285.....	5.6 days	ESO NTT, SOFI	K_s	61×60	1.25–1.42	20.5
2002 Aug 25.9389–26.0375.....	6.3 days	CA 3.5 m, Omega Prime	K'	105×60	1.53–1.17	19.5
2002 Sep 29.1181–29.1458.....	40.5 days	ESO VLT, ISAAC	K_s	30×60	1.67–1.19	21.5

^a Time after the burst; mean of the observing run.

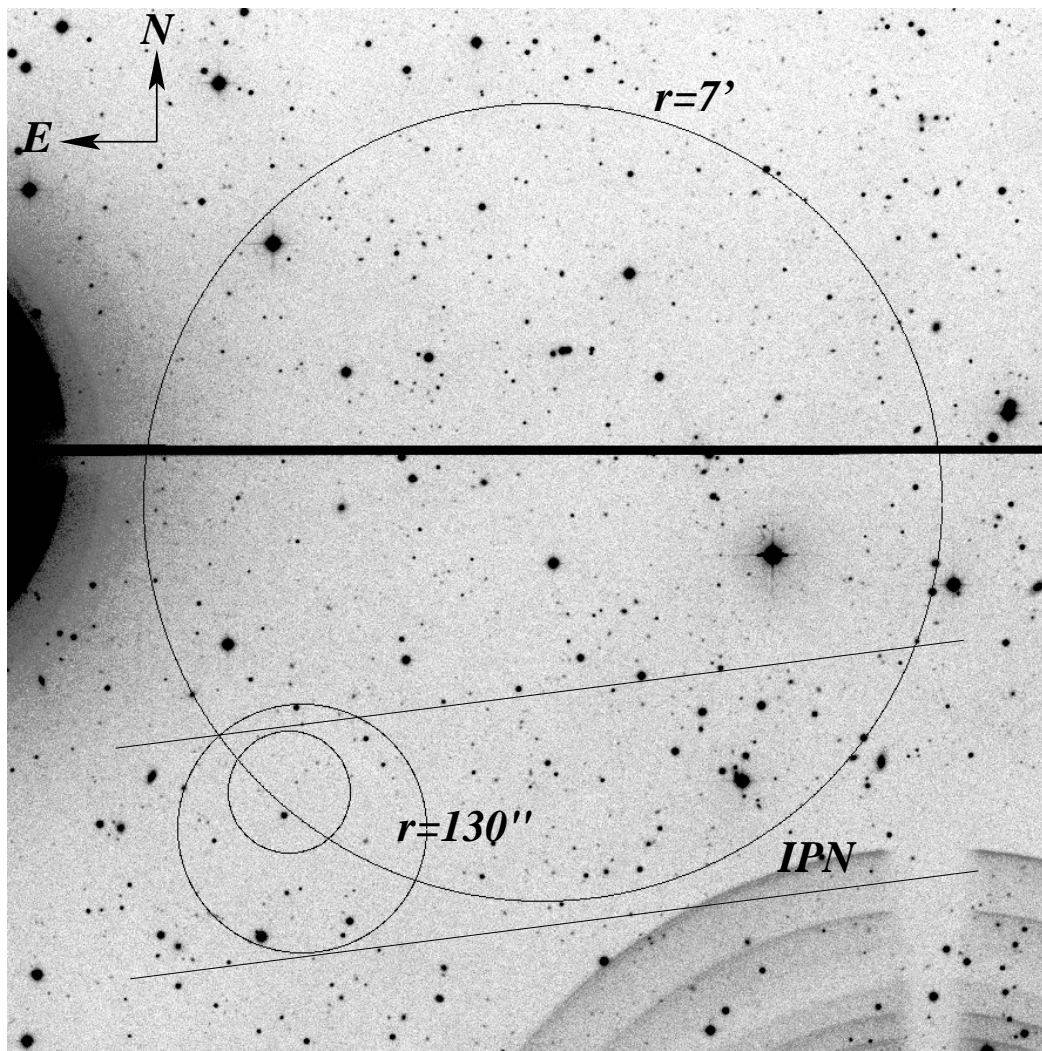


FIG. 1.—*R*-band image of the field of GRB 020819 taken with the Tautenburg Schmidt telescope one month after the burst. It illustrates the original $r = 7'$ *HETE* wide-field X-ray monitor (WXM) error circle, both *HETE*/*SXC* error circles (radius $130''$ and $64''$, respectively; Crew et al. 2002; Vanderspek et al. 2002), and the IPN annulus (Hurley et al. 2002; Crew et al. 2002). The *SXC* error circle agrees well with the IPN annulus. That the *SXC* error circle is close to the border of the WXM error circle is not unusual. This happened also for, e.g., GRB 021211. The bright star at left (Θ Psc) is responsible for the pattern at the lower right corner.

according to the air-mass coefficient provided on ESO's Web pages ($0.07 \text{ mag air mass}^{-1}$), although it is completely negligible for our purposes. The limiting magnitude of the Calar Alto images is typically $K' = 19.5$, whereas the combined ISAAC image is about 2 mag deeper (Fig. 3).

3. RESULTS

The data from the first Calar Alto run were reduced in the night when they were taken, and a search for a potentially bright transient NIR source was performed by a comparison with the Digitized Sky Survey¹⁴ but was not successful (§ 2). On the combined first epoch Calar Alto image only 14 sources with $K \lesssim 19.5$ are visible within the $64''$ *SXC* error circle. The second and third epoch Calar Alto data were then used to search for a fading *K*-band source. The photometry of some of these 14 sources on the Calar Alto images was affected by

scattered light from the bright star HD 220954 close to the error box (Fig. 2). Mainly this concerned the second observing run where those sources which were placed on a scattered light ray (Fig. 2) seemed to have brightened by 0.2–0.4 mag. Using SExtractor (Bertin & Arnouts 1996) and taking this scattered light effect into account did not reveal any fading source. In particular, no source disappeared. These 14 sources are listed in Table 2 together with their apparent magnitude and their morphological appearance on the deep, high-resolution ISAAC image. We note that the photometric calibration of the ISAAC data might be affected by an unreliable observation of a standard star (incorrect tracking of the telescope). Since this image is our deepest, we used it to set constraints on the *K*-band magnitude of the afterglow of GRB 020819. A comparison between the Calar Alto and the SOFI calibration has shown that an additional systematic error on the order of $\pm 0.2 \text{ mag}$ should be added to the errors listed in Table 2, which are the photometric errors calculated by SExtractor. This does not affect the following discussion in any way.

¹⁴ Available at <http://arch-http.hq.eso.org/~dss/dss>.

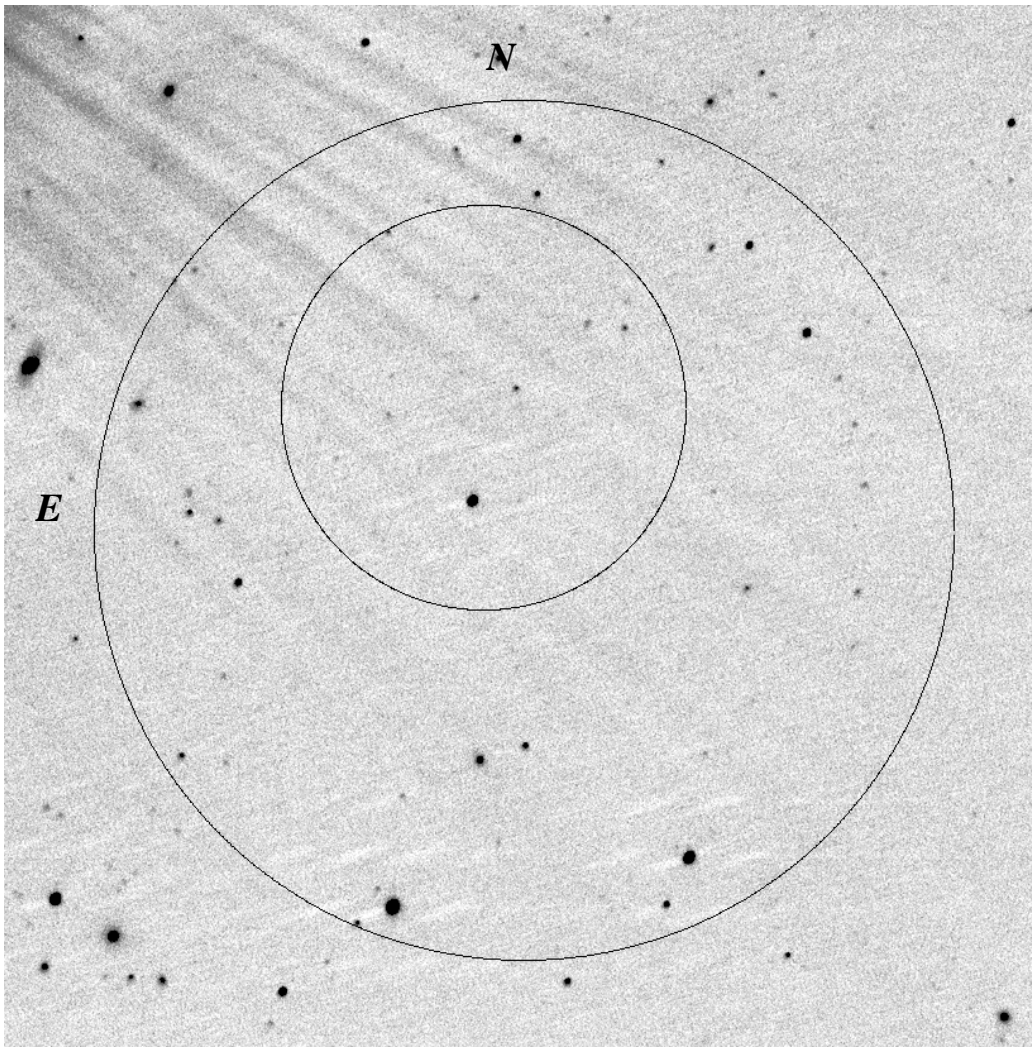


FIG. 2.—First epoch K' -band image of the GRB error box obtained 9 hr after the burst with the Calar Alto 3.5 m telescope. It shows the original and the revised *HETE/SXC* error circle (radius 130'' and 64'', respectively). The bright star Θ Psc = HD 220954 (spectral type K1 III) slightly affected the image at the upper left corner.

The field of GRB 020819 is at high Galactic latitude (-50°), so that the stellar density is low and any potential afterglow should have been easily detectable; i.e., crowding was not a likely cause for nondetection of the afterglow. Furthermore, according to *COBE*'s far-infrared all-sky survey, the Galactic visual extinction along the line of sight

through the Galaxy is only about 0.2 mag (Schlegel, Finkbeiner, & Davis 1998), so that extinction by Galactic dust is negligible in the K band. Although the angular resolution of the *COBE* maps is rather coarse, it is unlikely that at these Galactic latitudes a small and dense Galactic interstellar cloud is placed along the line of sight.

TABLE 2
OBJECTS IN THE ISAAC FIELD OF VIEW

Number	K_s	Class ^a	Number	K_s	Class ^a
1.....	17.86 ± 0.01	s	8.....	19.25 ± 0.03	e
2.....	19.41 ± 0.04	s	9.....	18.14 ± 0.02	e
3.....	17.65 ± 0.01	e	10.....	17.35 ± 0.01	s
4.....	19.21 ± 0.04	s	11.....	18.98 ± 0.04	e
5.....	18.88 ± 0.04	e	12.....	18.75 ± 0.02	s
6.....	17.60 ± 0.01	s	13.....	13.80 ± 0.01	s
7.....	17.37 ± 0.01	s	14.....	19.24 ± 0.04	s

NOTE.— See Fig. 3.

^a Morphological classification: s = stellar, e = extended.

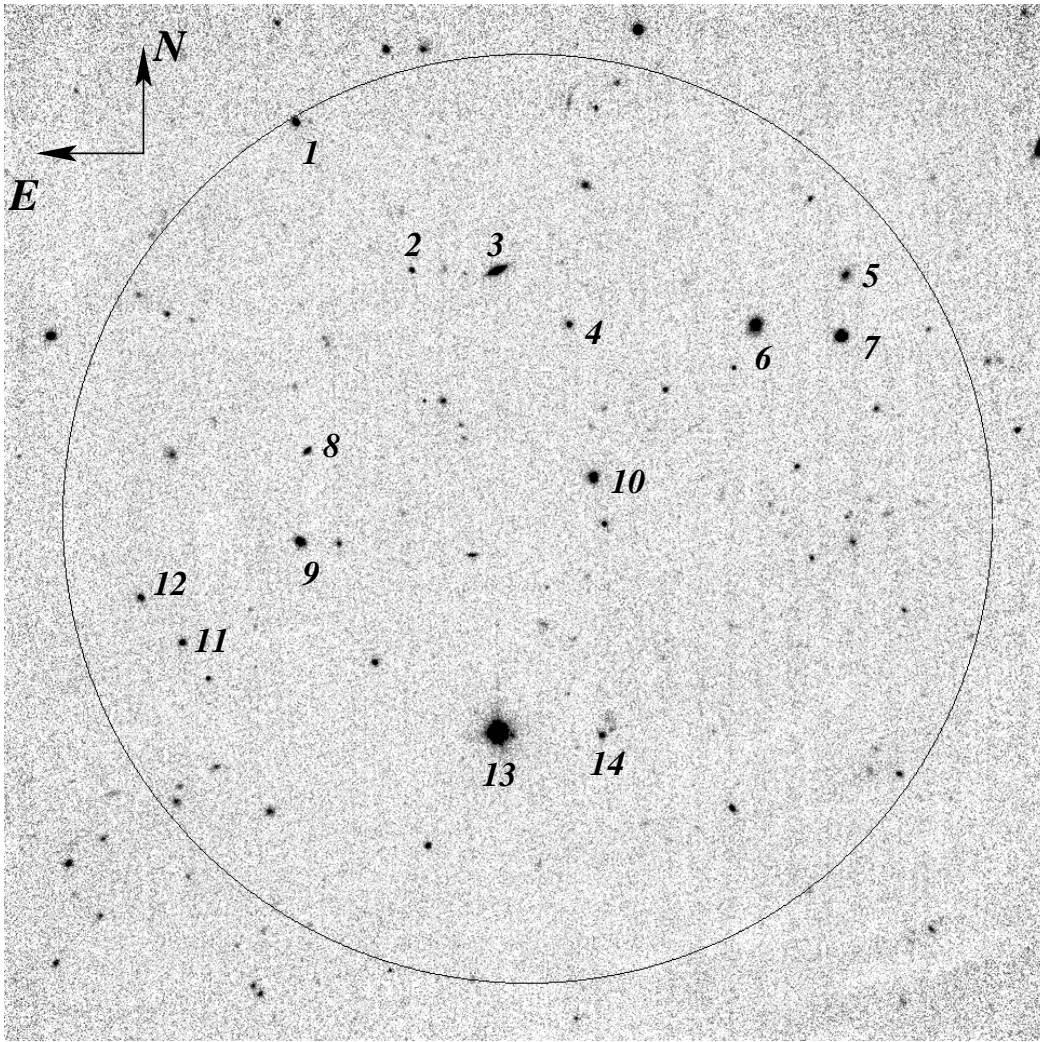


FIG. 3.—Deep ISAAC K_s -band image of the $64''$ SXC error circle. The K -band magnitudes of objects that are visible on the first epoch Calar Alto image are listed in Table 2.

4. DISCUSSION

4.1. *The Dust Extinction Hypothesis and GRB 020819*

Our data suggest that any afterglow of GRB 020819 was fainter than $K' = 19$ only 9 hr after the burst ($F_\nu < 17 \mu\text{Jy}$). This, together with its nondetection in deep and prompt optical searches down to $R \approx 20.5$ only 0.13 days after the burst (Price & McNaught 2002) and $R \approx 22.15$ at $t = 0.37$ days after the burst (Levan et al. 2002; for a compilation of all reports see Barthelmy et al. 1994 and J. Greiner's Web site),¹⁵ qualifies this burst as a dark burst. We stress that there is no general physical definition in the literature of the phrase “dark burst.” We use this phrase to mean that the afterglow was not detected down to faint flux levels in the optical/NIR bands allowing for the possibility that it was even fainter than the faintest optical/NIR afterglows discovered so far.

Our observations of the GRB 020819 field represent one of the deepest follow-up observations of a GRB ever performed in the K band within 12 hr after a burst (for a brief

summary, see Vreeswijk et al. 2000). In the following discussion we assume that the faintness of the afterglow was due to dust extinction in its host galaxy. First, we compare the observational upper limit to its K -band magnitude with the magnitudes of those optically detected GRB afterglows that were also followed up in the K band and have measured redshifts.¹⁶ This includes the bursts 971214 ($z = 3.42$), 980703 ($z = 0.97$), 991216 ($z = 1.02$; we assume here the reported lower limit to z ; Vreeswijk et al. 1999), 000301C ($z = 2.04$), 000926 ($z = 2.04$), and 011121 ($z = 0.36$). Although this set of bursts with K -band light curves is rather small, they cover a broad redshift range. Furthermore, their afterglows showed a different fading behavior and had different spectral energy distributions, and the derived physical properties of the medium surrounding the burster is different from burst to burst. In other words, the observational fact that GRB afterglows do not represent standard candles is implicit in our analysis. In the following we refer to these afterglows as reference afterglows. Second, we estimate a

¹⁵ See footnote 12.

¹⁶ We restrict ourselves to bursts observed before 2001 December to ensure that all observational data have been published at the time of writing of the present paper.

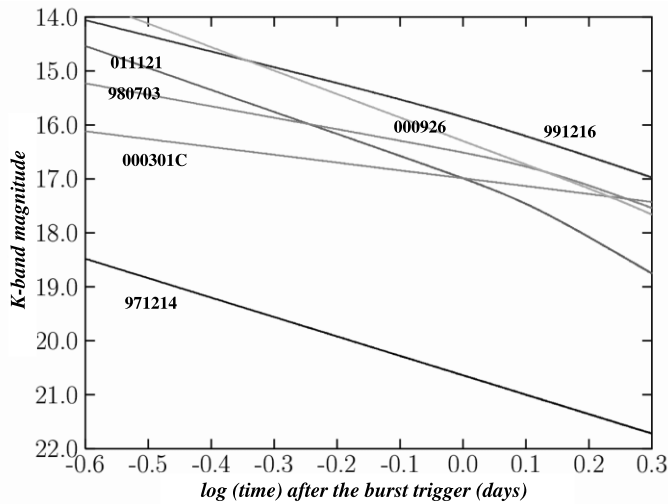


Fig. 4.— K -band light curves of the reference afterglows. The curves were calculated on the basis of photometric data published in the literature. The data are corrected for Galactic extinction and the contribution from the host galaxies to the magnitudes of the optical transients.

lower limit to the dust extinction in the host galaxy of GRB 020819 that may have obscured the afterglow of this burst.

None of our chosen reference afterglows has been observed in the K band 9 hr after the corresponding burst. Therefore, in order to predict their K -band magnitudes 9 hr after the burst, we calculated their light curves based on optical and NIR data available in the literature (Fig. 4). The conclusion we can then draw is how much fainter the afterglow of GRB 020819 was in the K band with respect to the reference afterglow at the same time Δt after the burst trigger. Naturally, this difference in magnitude could easily be caused by a different redshift alone. Since we cannot explore this hypothesis directly, we use these six reference bursts/afterglows to derive “statistical” conclusions based on the fact that these bursts are, to some degree, randomly selected from the entire GRB afterglow ensemble.

In doing so, at first we assumed that GRB 020819 was at the same redshift as the chosen reference burst. We then estimate the extinction by dust in the host galaxy of GRB 020819 required to make its afterglow nondetectable down to $K = 19$ only 9 hr after the burst, assuming that the physical properties of this afterglow resemble those of the reference afterglow. This procedure was then repeated for every one of the six reference bursts. The results are presented in Figure 5. Shown there is the manner in which extinction by cosmic dust in the GRB host galaxy can dim the apparent K -band magnitude of an afterglow. When calculating these curves, we made use of the compilation of analytic expressions for dust extinction curves by Reichart (2001) and used an extinction curve for the Large Magellanic Cloud (LMC; i.e., no 2200 Å bump) and a ratio of total-to-selective extinction of $R_V = 3.1$. Although there is ad hoc no reason for preferring the LMC extinction curve for GRB host galaxies, for the redshifts of our targets the observed K -band extinction is completely insensitive to the optical properties of the dust grains in the UV band. For the spectral energy distribution of the afterglow, $F_\nu \sim \nu^{-\beta}$, $\beta = 0.8$ was set. Finally, the definition of the filter response function was taken from Johnson (1965).

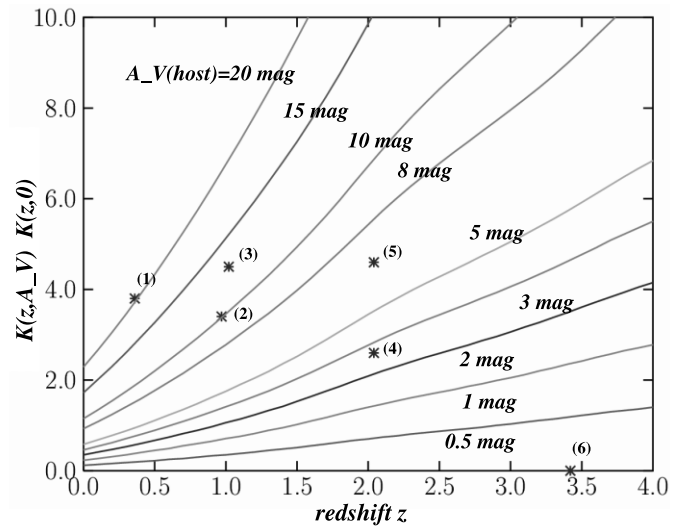


Fig. 5.—Shown here is the manner in which extinction by cosmic dust in the GRB host galaxy can affect the apparent magnitude of a GRB afterglow. The ordinate measures the magnitude difference in the K band between an extinguished afterglow and a nonextinguished afterglow at the same redshift z . This is shown for various amounts of the visual extinction $A_V(\text{host})$ in the host galaxy. Filled circles indicate constraints on the extinction by dust in the host galaxy of GRB 020819 assuming that the physical properties of the afterglow of this burst were identical to that of the following reference afterglows: (1) GRB 011121, (2) GRB 980703, (3) GRB 991216, (4) GRB 000301C, (5) GRB 000926, and (6) GRB 971214 (for details see text).

The visual extinction in the GRB host galaxy required in order to dim an afterglow in the K band increases rapidly with decreasing redshift (Fig. 5). If GRB 020819 would have been at $z = 0.36$ and the physical properties of its afterglow would have been identical to that one of GRB 011121, then more than 20 mag visual extinction is needed in the host galaxy of GRB 020819 in order to dim its afterglow by 3.8 mag in the K band. On the other hand, if GRB 020819 was $z \gtrsim 3.5$, no extinction by dust is required. The burst GRB 971214 was at $z = 3.42$, and its afterglow had approximately $K' = 19$ only 9 hr after the burst; i.e., it was as faint as the magnitude limit we can set for the afterglow of GRB 020819. Clearly, if GRB 971214 had not been detected in deep optical and NIR observations, it would also have been defined as a dark burst.

The conclusion we draw from this procedure is that only a modest visual extinction in the host galaxy, comparable to that which dimmed the afterglow of GRB 970828 (4 mag; Djorgovski et al. 2001), can easily have extinguished the afterglow of GRB 020819 even in the K band if its redshift was $\gtrsim 2$.

A deep optical upper limit ($R = 22.15$) was obtained 0.37 days after the burst (Levan et al. 2002), i.e., practically at the same time when the first Calar Alto K -band data were taken. Provided that there was no sharp break in the light curve of the afterglow of GRB 020819 between 4 and 9 hr after the burst, this is the deepest flux limit to the afterglow light curve in the R band. Following the same procedure as before we find the following: The potential R -band afterglow (AG) of GRB 020819 at $\Delta t = 9$ hr after the burst was 4.4 mag fainter in R than AG 011121, 1.7 mag fainter than AG 980703, 5.3 mag fainter than AG 991216, 2.9 mag fainter than AG 000301C, 4.5 mag fainter than AG 000926, and 0.6 mag fainter than AG 971214 (we have corrected

here the reported R -band upper limit of AG 020819 for a Galactic extinction of 0.15 mag in the R band, and we have subtracted the magnitudes of the host galaxies from the magnitudes of the reference afterglows). Assuming again that GRB 020819 was at the same redshift as the chosen reference burst and that the physical properties of its afterglow were identical to those of the reference afterglow we conclude the following. The visual extinction A_V (host) required in order to dim the potential R -band afterglow of GRB 020819 by these magnitudes is 3.9, 1.0, 3.2, 1.5, 2.3, and 0.3 mag, respectively. In other words, assuming for example that the physical properties of AG 020819 resembled those of AG 011121 and that GRB 020819 was at the same redshift as GRB 011121 ($z = 0.36$), then only a modest extinction of A_V (host) ≈ 4 mag would have been sufficient in order to dim AG 020819 by about 4.4 mag in the R band to $R > 22$ nine hours after the burst. But an A_V (host) of only 4 mag is not sufficient in order to dim AG 020819 in the K band at the same time by 3.8 mag, as we have found before. In order to do that, about 20 mag visual extinction is required, whereas an extinction of 4.4 mag would dim the afterglow in the K band by only 0.75 mag. In a similar way, in all but one case (GRB 971214) the K -band upper limit to AG 020819 provides stronger constraints on A_V (host) than do the optical upper limits.

4.2. The Dust Extinction Hypothesis and the Ensemble of the K -Band Dark Bursts

In order to put our conclusions concerning GRB 020819 into broader context, we have checked the literature for similar cases of K -band dark afterglows. In doing so, we have selected from the compilation of J. Greiner¹⁷ and from the data base of the Gamma-Ray Burst Coordinated Network Circular (GCN; Barthelmy et al. 1994) all those dark bursts that have not been discovered in the optical *as well as* in the

K band, in spite of response times of the K -band observations of $\lesssim 2$ days, deep NIR flux limits, and small GRB error boxes. These data are summarized in Table 3 and in the Appendix. In Table 3 again Δt is the time after the burst in days, and K_{lim} is the limiting magnitude reported in the GCN. Also given are the Galactic coordinates based on B1950 and the color index $E(B-V)$ along the line of sight through the Galaxy, calculated according to the maps of Schlegel et al. (1998).

Following the same procedure as in the case of GRB 020819 (§ 4.1), we can use the reported K -band upper limits on the afterglows of the bursts listed in Table 3 in order to calculate what the required extinction A_V (host) in their host galaxies would have been in order to make them dark in the K band at the corresponding times Δt after the bursts. The deduced amount of extinction A_V (host) in the host galaxies of the K -band dark bursts is summarized in Table 4. On the basis of these results, we conclude that there is no need for very high redshifts in order to make GRB afterglows dark in the K band between 0.3 and ≈ 2 days after a burst. Although we cannot exclude that high redshift, internal physics, and/or different populations of bursters come into play here, we can state that dust extinction alone can explain the observational data for K -band dark bursts/afterglows, *if these bursts were at modest redshifts* (say, $z = 2-3$). A combination of only a modest extinction with a modest redshift can in all cases explain the nondetection in the K band of the GRB afterglows listed in Table 3. In all investigated cases, an extinction of ~ 1 mag for a host at redshift of 3 would have been sufficient to make all afterglows listed in Table 3 dark in the K band. And in most cases an extinction of 4 mag for a host at a redshift around $z = 2$ can do the same also. These are numbers that are not extraordinarily large with respect to what is known so far about redshifts and extinctions of the optically dark afterglows of GRB 970828 [A_V (host) ≥ 0.8 mag; Djorgovski et al. 2001], GRB 980329 (2.8 mag if $z = 1$; Yost et al. 2002), and GRB 000210 (0.9–3.2 mag if $z = 0.85$; Piro et al. 2002). Furthermore, this

¹⁷ See footnote 12.

TABLE 3
K-BAND DARK GRB AFTERGLOWS ORDERED ACCORDING TO THE RESPONSE TIME Δt (days)

GRB	(l , b) ^a (deg)	$E(B-V)$ ^b	Δt	K_{lim} ^c	GCN Number ^d
020819	88.54, -50.89	0.07	0.37	19.0	1510
0.02 001109	84.23, 24.96	0.04	0.40	19.9	886
0.01 020812	40.71, -26.29	0.06	0.51	17.0	1499
0.02 011030	110.95, 20.66	0.39	0.52	18.9	1142 ^e
020321	308.18, -23.02	0.10	0.61	18.9	1314
0.03 000615	109.58, 38.82	0.02	0.71	18.0	713 ^f
010220	135.08, 1.41	0.85	0.97	17.2	979
0.29 991014	202.54, 5.18	0.26	1.24	19.0	none
0.09 000214	329.08, -25.00	0.06	1.35	18.1	564
0.02 991106	102.55, -2.58	0.71	1.37	18.8	446
0.24 020418	263.12, -9.69	0.26	1.61	20.9	1419

^a Either the central coordinate of the GRB error box or the coordinate of the potential radio or X-ray afterglow.

^b According to the maps of Schlegel et al. 1998.

^c Formally, we have corrected published K -band limits for the Galactic extinction; however, this correction is in all cases rather small and surely completely covered by the reported *estimated* upper limits.

^d See the GCN Web page at <http://gcn.gsfc.nasa.gov/gcn/>.

^e Reported K_{lim} corrected to $K_{\text{lim}} \approx 19$.

^f Reported K_{lim} corrected to $K_{\text{lim}} \approx 18$.

TABLE 4
LOWER LIMITS TO THE EXTINCTION $A_V(\text{HOST})$ [mag] REQUIRED IN ORDER TO DIM THE AFTERGLOWS

GRB	011121 $z = 0.36$	980703 $z = 0.97$	991216 $z = 1.02$	000301C $z = 2.04$	000926 $z = 2.04$	971214 $z = 3.42$
020819	20.3	10.1	12.7	3.7	6.5	0.0
001109	24.6	12.6	15.1	4.9	7.7	0.6
020812	6.4	3.2	5.8	0.6	2.8	0.0
011030	16.5	8.8	11.2	3.3	5.4	0.0
020321	14.9	8.4	10.6	3.1	5.0	0.0
000615	8.6	5.3	7.4	1.7	3.3	0.0
010220	1.4	2.1	3.9	0.3	1.3	0.0
991014	8.3	6.6	7.9	2.6	3.2	0.0
000214	2.4	3.6	5.0	1.3	1.7	0.0
991106	5.9	5.6	6.9	2.3	2.7	0.0
020418	14.8	11.1	12.3	5.1	5.2	0.0

NOTES.—All data are corrected for Galactic extinction (see Table 3). More precisely, listed here is the amount of extinction in addition to any extinction that affected the reference afterglows (0.38 ± 0.1 mag for GRB 971214; Galama & Wijers 2001; 1–2 mag for GRB 980703; Berger, Kulkarni, & Frail 2001; 0 mag for GRB 011121; Greiner et al. 2003)

matches well into the context that some GRB afterglows have been found to be affected by dust extinction in their host galaxies with $A_V(\text{host}) \lesssim 2$ mag (e.g., GRB 980703, Castro-Tirado et al. 1999; GRB 000418, Klose et al. 2000).

There are at least two other methods to estimate the visual extinction in a GRB host galaxy if X-ray data of an afterglow are available. The first makes use of the deduced hydrogen column density N_H along the line of sight to the X-ray source. The other requires adopting a light curve and a spectral energy distribution of the afterglow between the X-ray band and the optical bands. Since this introduces further assumptions about the afterglow light, we only considered the first method. For three of the bursts listed in Table 3, limits on the hydrogen column density N_H along the line of sight to the afterglow have been published in the literature (GRB 991014, in 't Zand et al. 2000; GRB 000214, Antonelli et al. 2000; GRB 010220, Watson et al. 2002). Performing the standard approach (cf. Groot et al. 1998), for GRB 010220 we arrive at rather large possible values for $A_V(\text{host})$ ($\lesssim 25$ mag if $z = 1$ and $N_H = 1.6 \times 10^{22}$; see the Appendix) but get weaker estimates for GRB 991014 [$A_V(\text{host}) \lesssim 8$ mag if $z \lesssim 0.4$] and GRB 000214 [$A_V(\text{host}) \lesssim 0.5$ mag if $z \sim 0.4$]. The latter two results are in qualitative agreement with our estimates on $A_V(\text{host})$ based on the K -band upper limits. The former result might be affected by the assumption of a collisionally ionized plasma model to estimate N_H (Watson et al. 2002).

4.3. The Dust Extinction Hypothesis and Low- z Dark Bursts

If the K -band dark afterglows we have investigated here (Table 3) would have been placed at comparable low redshifts, say at $0.3 \lesssim z \lesssim 1$, and if their unobscured luminosities would have been identical to those of the reference afterglows, then the visual extinction $A_V(\text{host})$ required in the GRB hosts in order to obscure these afterglows is very large. For up to 50% of all investigated dark bursts (Table 3) it exceeds 10 mag (Table 4). Consequently, if the redshift distribution of the dark bursts follows the redshift distribution of those bursts with detected optical afterglows (with a peak around $z = 1$), then the dust extinction hypothesis requires a considerable fraction of GRBs to occur in very obscured star-forming regions. This raises the question about the

circumstances under which a GRB afterglow could remain dark in the K band in spite of the dust destruction by the intense gamma-ray burst, the potential UV flash accompanying this burst, and the intense, long-lasting fireball light. Theoretical investigations suggest that dust can be destroyed by a GRB out to a radius of several parsecs, assuming the burster is located in a typical molecular cloud (e.g., Waxman & Draine 2000; Fruchter, Krolik, & Rhoads 2001). If the GRB explosion is not able to burn a dust-free hole into the interstellar cloud in which it is placed, then this might require a very compact and/or possibly very extended opaque star-forming region (Venemans & Blain 2001). This is not an unusual scenario since such super-dense star-forming regions do exist even in the local universe (e.g., Hunt, Vanzi, & Thuan 2001). Finally, we note in passing that observations of afterglows in the soft X-ray band could help to reveal if a burster is located close to a dusty star-forming region (Klose 1998).

The other possibility to block the intense fireball light is a *globally* very dusty starburst galaxy. Observations indicate that the more powerful starbursts are hosted in dustier galaxies. The starburst galaxy Arp 220, for example, is heavily extinguished with $A_V = 15\text{--}45$ mag (e.g., Calzetti 2001). Heavily extinguished hosts point to submillimeter-bright galaxies as potential GRB hosts (for a discussion, see, e.g., Ramirez-Ruiz, Trentham, & Blain 2002). Observations indicate, however, that submillimeter-bright hosts are generally absent in error boxes of dark bursts (Barnard et al. 2003; Berger et al. 2002b; but see also Castro Cerón et al. 2003). It seems that this is difficult to reconcile with the dust extinction hypothesis of the dark bursts; however, the data base is still poor.

5. CONCLUDING REMARKS

Extinction by cosmic dust in the GRB host galaxy could explain why the afterglow of GRB 020819 remained undetected down to faint flux levels even in the K band 9 hr after the burst. In general, we find that the dust extinction hypothesis leads to results that match what is known so far about redshifts and extinctions of *optically detected* GRB afterglows. In particular, in order to explain K -band dark bursts, there is no need for very large redshifts. On the other

hand, large amounts of extinction would be required in order to dim the afterglows if the dark bursts are at low redshifts. This could be evidence that a considerable fraction of the dark afterglows might not be dark in the optical/NIR bands because of extinction by cosmic dust in their host galaxies but because of intrinsic low luminosity, a conclusion also drawn by others (Fynbo et al. 2001; Hjorth et al. 2002; Lazzati, Covino, & Ghisellini 2002; Taylor et al. 2000). Indeed, a number of GRB progenitor scenarios have been discussed for GRBs in the literature (e.g., Fryer, Woosley, & Hartmann 1999), and some of them suggest the existence of *intrinsically* low-luminous afterglows.

Whatever the nature of the dark bursts is, it is nevertheless surprising that after 5 years of intense GRB follow-up observations world-wide, no afterglow has been detected that was “Lyman dropped-out” at optical wavelengths below $0.9 \mu\text{m}$ but visible in the near-infrared.¹⁸ The predicted large population of high- z bursts based on *BATSE* gamma-ray data alone (for a discussion, see, e.g., Mészáros et al. 2003) has either been hidden thus far by an observational bias or it does not exist in this predicted large amount at all. A final observational consensus about the nature of the dark bursts might not be at hand until rapid follow-up NIR

¹⁸ The most distant GRB afterglow observed so far was at $z = 4.5$ (GRB 000131; Andersen et al. 2000) and Lyman dropped-out in the R band.

observations of GRB error boxes by robotic telescopes are technically feasible. Theory predicts that minutes after a burst, afterglows reach their luminosity maximum with several magnitudes brighter than 1 day later (e.g., Panaitescu & Kumar 2001). Dedicated fully robotic NIR telescopes, like the REM telescope (Zerbi et al. 2001) or the upgraded Super-LOTIS telescope (Park et al. 1999), will bring us a big step forward in tackling the issue of the dark bursts.

This work was based on data obtained on the German-Spanish Astronomical Centre, Calar Alto, operated by the Max-Planck-Institut for Astronomy, Heidelberg, jointly with the Spanish National Commission for Astronomy. It has profited from the GCN data base at NASA maintained by Scott Barthelmy, NASA. This paper is partly based on observations collected at the European Southern Observatory, La Silla and Paranal, Chile (ESO Programme 165.H-0464). We thank the observers and the staff at ESO for performing the SOFI and the ISAAC observations. This study has made use of the SIMBAD database, operated at CDS, Strasbourg, France. S. K. acknowledges helpful comments by Johan Fynbo, Jens Hjorth, Attila Mészáros, Holger Pedersen, and Paul Vreeswijk. J. M. C. C. acknowledges the receipt of a FPI doctoral fellowship from Spain’s Ministerio de Ciencia y Tecnología. We thank an anonymous referee for a prompt and very helpful reply.

APPENDIX A

NOTES ON INDIVIDUAL BURSTS IN TABLE 3

GRB 991014.—X-ray afterglow detected by *BeppoSAX*, error box size $\approx 4 \text{ arcmin}^2$. The X-ray observation constrains the hydrogen column density as $N_{\text{H}} \lesssim 8.6 \times 10^{21} \text{ cm}^{-2}$, whereas the Galactic value is $2.5 \times 10^{21} \text{ cm}^{-2}$ (in ’t Zand et al. 2000); $R > 23.1$ at $\Delta t = 11.2 \text{ hr}$ (GCN 423); no radio afterglow has been detected (GCN 425).

GRB 991106.—X-ray afterglow detected by *BeppoSAX*, error circle $r = 1'5$ (GCN 445), but the status of the X-ray source is not clear (GCN 448). No deduced value for N_{H} has been published; the burst occurred at low Galactic latitude, the Galactic visual extinction is therefore high (Table 3); unfiltered images give $m > 13.4$ at $\Delta t = 3 \text{ minutes}$ (GCN 437); $R > 21$ at $\Delta t = 7.7 \text{ hr}$ (GCN 438); $R > 20$ at $\Delta t = 9.2 \text{ hr}$ (GCN 436); $R > 22$ at $\Delta t = 10 \text{ hr}$ (GCN 440); $I > 22$ at $\Delta t = 9.6 \text{ hr}$ (GCN 447); potential radio afterglow discovered (GCN 444); the K -band observations include the position of this radio counterpart but do not show any NIR counterpart.

GRB 000214.—X-ray afterglow detected by *BeppoSAX*, error circle $r = 50''$. A potential Fe $K\alpha$ emission line points to a redshift of $z = 0.37\text{--}0.47$ (Antonelli et al. 2000); the X-ray observation constrains the hydrogen column density as $N_{\text{H}} = 0.7_{-0.7}^{+7.5} \times 10^{20} \text{ cm}^{-2}$, whereas the Galactic value is $5.5 \times 10^{20} \text{ cm}^{-2}$. No radio afterglow has been detected (GCN 562); no optical follow-up observations have been reported.

GRB 000615.—X-ray afterglow detected by *BeppoSAX*, error circle $r = 1'5$ but its status is not clear (GCN 707). No X-ray afterglow data have been published; no radio afterglow has been detected (GCN 721); $R > 20$ at $\Delta t = 4.5 \text{ hr}$ (GCN 706); $R > 21.5$ at $\Delta t = 22 \text{ hr}$ (GCN 709).

GRB 001109.—X-ray afterglow detected by *BeppoSAX*; error circle $r = 50''$ (GCN 885). No deduced value for N_{H} published; $R > 21.5$ at $\Delta t = 9 \text{ hr}$, $I > 22.9$ at $\Delta t = 11.4 \text{ hr}$ (Castro Cerón et al. 2003); an originally claimed radio afterglow (GCN 880) was later not confirmed (GCN 1168).

GRB 010220.—Detected by *BeppoSAX*, error circle $r = 4'$ (GCN 959). *XMM-Newton* observation of the X-ray afterglow; a redshift of $z \sim 1$ gives a best fit to the X-ray data; best fit for a collisionally ionized plasma model gives $N_{\text{H}} = 16 \times 10^{21} \text{ cm}^{-2}$ compared to the Galactic value of $8.6 \times 10^{21} \text{ cm}^{-2}$ (Watson et al. 2002); the position of a potential radio afterglow (GCN 958) does not coincide with the position of the assumed X-ray afterglow by Watson et al. (2002); $R > 23.5$ at $\Delta t = 0.35 \text{ days}$ (GCN 958); $R > 23$ at $\Delta t = 28 \text{ hr}$ (GCN 1001).

GRB 011030.—X-ray-rich GRB (GCN 1138); X-ray afterglow detected by *BeppoSAX*, error circle $r = 2'1$ (GCN 1123); a power-law model with a Galactic absorption is an acceptable fit to the data (GCN 1143); $R > 21$ at $\Delta t = 7 \text{ hr}$ (GCN 1120); the K -band observations cover only 90% of the GRB error circle include, however, the position of a potential radio and X-ray transient (GCNs 1136, 1143, 1268); the potential host galaxy is at $z \lesssim 3$ (GCN 1268).

GRB 020321.—X-ray afterglow detected by *BeppoSAX*, error circle $r = 2'$ (GCN 1285); *XMM-Newton* (GCN 1348) and *Chandra* (GCN 1342) X-ray observations; the status of the *BeppoSAX* X-ray afterglow is not clear (GCN 1348). The burst occurred at low Galactic latitude; the Galactic visual extinction is therefore high (Table 3); $R > 19$ at $\Delta t = 8.2 \text{ hr}$; $R > 20.5$ at

$\Delta t = 0.4$ days (GCN 1289); $R > 24$ at $\Delta t \sim 1$ day (GCN 1305); several optical afterglow candidates have been proposed in the literature; no radio follow-up observations have been reported.

GRB 020418.—Burst localized by the IPN, error box size 20 arcmin², $r = 5'$ circumscribing circle (GCN 1376); the K -band observations cover only 60% of the GRB error box (GCN 1419); $R > 21.2$ at $\Delta t = 25.5$ hr (GCN 1379); neither X-ray nor radio follow-up observations have been reported.

GRB 020812.—Error box size $10' \times 25'$ rectangle (GCN 1468); $R > 18$ on combined images taken at $\Delta t = 28$ minutes until 3 hr after the burst (GCN 1469); the K -band observations cover only 40% of the error box; neither X-ray nor radio follow-up observations have been reported.

REFERENCES

- Andersen, M. I., et al. 2000, *A&A*, 364, L54
 Antonelli, L. A., et al. 2000, *ApJ*, 545, L39
 Bagoly, Z., Csabai, I., Mészáros, A., Mészáros, P., Horváth, I., Balázs, L. G., & Vavrek, R. 2003, *A&A*, 398, 919
 Barnard, V. E., et al. 2003, *MNRAS*, 338, 1
 Barraud, C., et al. 2003, *A&A*, 400, 1021
 Barthelmy, S., et al. 1994, in *AIP Conf. Proc. 307, Gamma-Ray Bursts: Second Huntsville Gamma-Ray Burst Workshop*, ed. J. Fishman, J. J. Brainerd, & K. Hurley (New York: AIP 643)
 Berger, E., Kulkarni, S. K., & Frail, D. A. 2001, *ApJ*, 560, 652
 Berger, E., et al. 2002a, *ApJ*, 581, 981
 ———. 2003, *ApJ*, 588, 99
 Bertin, E., & Arnouts, S. 1996, *A&AS*, 117, 393
 Calzetti, D. 2001, *PASP*, 113, 1449
 Castro Cerón, J. M., et al. 2003a, *A&A*, submitted
 ———. 2003b, in *AIP Conf. Proc. 662, Gamma-Ray Burst and Afterglow Astronomy 2001: A Workshop Celebrating the First Year of HETE Mission*, ed. G. R. Ricker & R. K. Vanderspek (New York: AIP), 424
 Castro-Tirado, A. J., et al. 1999, *ApJ*, 511, L85
 Crew, G., et al. 2002, *GCN Circ.* 1526 (<http://gcn.gsfc.nasa.gov/gcn/gcn3/1526.gcn3>)
 Devillard, N. 1997, *Messenger*, 87, 19
 Djorgovski, S. G., et al. 2001, *ApJ*, 562, 654
 Frail, D. A., & Berger, E. 2003, *GCN Circ.* 1842 (<http://gcn.gsfc.nasa.gov/gcn/gcn3/1842.gcn3>)
 Fruchter, A., Krolik, J. H., & Rhoads, J. E. 2001, *ApJ*, 563, 597
 Fryer, C. L., Woosley, S. E., & Hartmann, D. H. 1999, *ApJ*, 526, 152
 Fynbo, J. U., et al. 2001, *A&A*, 369, 373
 Galama, T. J., & Wijers, R. A. M. J. 2001, *ApJ*, 549, L209
 Greiner, J., et al. 2003, *A&A*, submitted
 Groot, P. J., et al. 1998, *ApJ*, 493, L27
 Henden, A. A., et al. 2002, *GCN Circ.* 1510 (<http://gcn.gsfc.nasa.gov/gcn/gcn3/1510.gcn3>)
 Hjorth, J., et al. 2002, *ApJ*, 576, 113
 Horváth, I., Mészáros, P., & Mészáros, A. 1996, *ApJ*, 470, 56
 Hunt, L. K., Vanzi, L., & Thuan, T. X. 2001, *A&A*, 377, 66
 Hurley, K., et al. 2002, *GCN Circ.* 1507 (<http://gcn.gsfc.nasa.gov/gcn/gcn3/1507.gcn3>)
 in 't Zand, J. J. M., et al. 2000, *ApJ*, 545, 266
 Johnson, H. L. 1965, *ApJ*, 141, 923
 Klose, S. 1998, *ApJ*, 507, 300
 Klose, S., et al. 2000, *ApJ*, 545, 271
 Lamb, D. Q., & Reichart, D. E. 2000, *ApJ*, 536, 1
 Lazzati, D., Covino, S., & Ghisellini, G. 2002, *MNRAS*, 330, 583
 Levan, A., et al. 2002, *GCN Circ.* 1517 (<http://gcn.gsfc.nasa.gov/gcn/gcn3/1517.gcn3>)
 Mészáros, A., & Mészáros, P. 1996, *ApJ*, 466, 29
 Mészáros, A., et al. 2003, in *Proc. Rome 2002 GRB Workshop*
 Paczyński, B. 1998, *ApJ*, 494, L45
 Panaitescu, A., & Kumar, P. 2001, *ApJ*, 554, 667
 Park, H.-S., et al. 1999, *A&AS*, 138, 577
 Pedersen, H., et al. 1998, *ApJ*, 496, 311
 Persson, S. E., et al. 1998, *AJ*, 116, 2475
 Piro, L., et al. 2002, *ApJ*, 577, 680
 Price, P. A., & McNaught, R. 2002, *GCN Circ.* 1506 (<http://gcn.gsfc.nasa.gov/gcn/gcn3/1506.gcn3>)
 Price, P. A., et al. 2002, *GCN Circ.* 1511 (<http://gcn.gsfc.nasa.gov/gcn/gcn3/1511.gcn3>)
 Ramirez-Ruiz, E., Trentham, N., & Blain, A. W. 2002, *MNRAS*, 329, 465
 Reichart, D. E. 2001, *ApJ*, 553, 235
 Rol, E., et al. 2002, *GCN Circ.* 1512 (<http://gcn.gsfc.nasa.gov/gcn/gcn3/1512.gcn3>)
 Schaefer, B. E., Deng, M., & Band, D. L. 2001, *ApJ*, 563, L123
 Schlegel, D., Finkbeiner, D., & Davis, M. 1998, *ApJ*, 500, 525
 Schmidt, M. 2001, *ApJ*, 552, 36
 Taylor, G. B., et al. 2000, *ApJ*, 537, L17
 van Paradijs, J., Kouveliotou, C., & Wijers, R. A. M. J. 2000, *ARA&A*, 38, 379
 van Paradijs, J., et al. 1997, *Nature*, 386, 686
 Vanderspek, R., et al. 2002, *GCN Circ.* 1508 (<http://gcn.gsfc.nasa.gov/gcn/gcn3/1508.gcn3>)
 Venemans, B. P., & Blain, A. W. 2001, *MNRAS*, 325, 1477
 Vrba, F. J., Hartmann, D. H., & Jennings, M. C. 1995, *ApJ*, 446, 115
 Vreeswijk, P. M., et al. 1999, *GCN Circ.* 496 (<http://gcn.gsfc.nasa.gov/gcn/gcn3/496.gcn3>)
 ———. 2000, *GCN Circ.* 886 (<http://gcn.gsfc.nasa.gov/gcn/gcn3/886.gcn3>)
 Watson, D., et al. 2002, *A&A*, 393, L1
 Waxman, E., & Draine, B. T. 2000, *ApJ*, 537, 796
 Yost, S. A., et al. 2002, *ApJ*, 577, 155
 Zerbi, F. M., et al. 2001, *Astron. Nachr.*, 322, 275